



King Saud University

**Journal of Saudi Chemical Society**

[www.ksu.edu.sa](http://www.ksu.edu.sa)  
[www.sciencedirect.com](http://www.sciencedirect.com)



## ORIGINAL ARTICLE

# Kinetics, mechanistic and synergistic studies of Alpha lipoic acid with hydrogen peroxide



Maria Taj Muhammad, M. Nasiruddin Khan \*

*Department of Chemistry, University of Karachi, Karachi 75270, Pakistan*

Received 14 November 2014; revised 15 January 2015; accepted 27 January 2015

Available online 11 February 2015

## KEYWORDS

Alpha lipoic acid;  
 Hydrogen peroxide;  
 Synergism;  
 Oxidation;  
 Reaction mechanism

**Abstract** Alpha lipoic acid (ALA) holds redox behavior that was observed in the presence of different metals utilizing hydrogen peroxide ( $\text{H}_2\text{O}_2$ ) as a strong oxidizing agent. The effects of different parameters like temperature, pH and concentrations were also monitored.

ALA in the presence of hydrogen peroxide ( $\text{H}_2\text{O}_2$ ) showed oxidation as well as degradation processes. To monitor the oxidation kinetics of ALA in the presence of different essential metals to find its reaction pathway using salt affect parameters.

The redox behavior of Alpha lipoic acid (ALA) was found to be significant at pH ranging from 4 to 10, at 29 °C in a given pseudo first order reaction conditions. The values of the rate constant in the presence of different essential metals such as Mo, Se, Co, Cr, Fe, and Zn were also obtained. Furthermore, synergistic effects were observed in the presence of  $\text{Mo}^{6+}$  and  $\text{Fe}^{2+}$  at all applied conditions.

Activation energy of ALA oxidation is 36.7 kJ whereas in the presence of  $\text{Fe}^{2+}$  its activation energy went up to 48 kJ; however, in the presence of  $\text{Mo}^{6+}$  the activation energy drops to 18.3 kJ. In the presence of  $\text{Fe}^{2+}$  and  $\text{Mo}^{6+}$  the synergistic effect works and its activation energy became 36.5 kJ. The reaction mechanism was also proposed.

© 2015 The Authors. Production and hosting by Elsevier B.V. on behalf of King Saud University. This is an open access article under the CC BY-NC-ND license (<http://creativecommons.org/licenses/by-nc-nd/4.0/>).

## 1. Introduction

Alpha lipoic acid (ALA) derives its name because of its higher degree of solubility in lipid and its acidic nature ( $\text{pK}_a = 4.7$ ). It helps in a number of in vivo reactions, like in a transfer of

hydrogen and acyl groups in oxidative decarboxylation of  $\alpha$ -keto acids. ALA acts as the chelator for metal in lead toxicity [1].

ALA and its reduced fellow di-hydro alpha lipoic acid (DHLA) hold all the necessary characteristics of an ideal anti-oxidant such as early quenching of free radicals, [2] chelate metals have an amphiphilic nature with no side effects [3]. Within the time period of 30–60 min maximum absorption was achieved when its single dose of 50–600 mg was administered [4].

ALA and DHLA are not only potent quenchers but also quench different oxygen species [1]. ALA neutralizes free radicals such as free OH, hypochlorous acid, singlet oxygen, but

\* Corresponding author. Tel.: +92 3142134934.

E-mail address: [nasiruk@uok.edu.pk](mailto:nasiruk@uok.edu.pk) (M.N. Khan).

Peer review under responsibility of King Saud University.



Production and hosting by Elsevier

not hydrogen peroxide [5]. ALA and DHLA, hold an ability to reduce oxidative stress by regenerating other antioxidants (vitamins C, E and glutathione), serving as a Reactive Oxygen Species (ROS) scavenger, and also chelate transition metals (Cu and Fe) [6,7]. Preferential metals being chelated by ALA and DHLA are  $\text{Cu}^{+2}$ ,  $\text{Zn}^{+2}$ , and  $\text{Pb}^{+2}$  whereas  $\text{Fe}^{+3}$  is chelated by DHLA only [8]. ALA when supplied exogenously shows its antioxidant properties and prevents the cause of damage due to ROS [1]. On the other hand  $\text{H}_2\text{O}_2$  is an environmentally friendly oxidizing agent due to the presence of only hydrogen and oxygen atoms which promotes the photo-catalysis in two possible ways;

1. Hydroxyl free radicals produced by  $\text{H}_2\text{O}_2$  reduction at the conduction band.
2. Hydroxyl radical produced by photolytic cleavage in the presence of UV radiations [9]. It is having many physiological and non-physiological uses so its trace concentration determination is also very important [10].

Iron an abundant metal in human physiology is redox active in nature and has great potential to generate free radicals mediated by Fenton chemistry. In aqueous medium ferrate is an energetic oxidizing agent, where its oxidation potential ranges from 2.20 V in acidic medium to 0.7 V in basic medium [11].  $\text{H}_2\text{O}_2$  plays a vital role in the death of osteoblast which is sensitive against ROS [12]. Among the elements, iron holding a redox active properties, exacerbates oxidative stress by OH generation by Fenton chemistry, ALA chelation with Fe in vivo has not been determined as yet [1]. Cells convert ALA into DHLA which in-turn can interact with Fe, although Fe chelation in vitro is possible with both ferric and ferrous.

The aim of the study was to find the kinetic aspects of ALA at various kinetic conditions. The behavior of ALA on the interaction with redox active specie ( $\text{H}_2\text{O}_2$ ), and then to see its oxidation behavior in the presence of different metals with

which it can easily interact. Software was used to prove the scavenging and synergistic properties on the described reaction.

## 2. Material and methods

### 2.1. Equipment

All the absorbance was recorded with a path length of 1 cm quartz cuvette using UV-Visible Spectrophotometer UV-1601 Shimadzu Japan. pH was adjusted by the help of a pH meter (Precisa 900) with accuracy of  $\pm 0.003$  pH. Temperature was maintained by using Memmert water bath (WB 14) with accuracy of  $\pm 0.1$  K.

### 2.2. Chemicals

Hydrogen peroxide ( $\text{H}_2\text{O}_2$ ) of Riedel-de Haën and for a pH maintenance, Hydrochloric acid (HCl) of REANAL and sodium hydroxide (NaOH) of Alpha aesar were used. lipoic acid and all metal salts of Sigma Aldrich, were purchased from a local supplier of Analytical Grade (AG). All the chemicals were used directly as received bases without purification. The Compusyn software was used for analyzing the combined effects of Fe and Mo on the reaction and reported in Table 1. The symbols Fa and CI represent, Fraction affected and Combination Index respectively.  $\text{CI} > 1$  means the combination effect is antagonistic in nature while  $\text{CI} = 1$  means it is an additive, whereas  $\text{CI} < 1$  shows synergism.

### 2.3. Procedure

ALA is almost insoluble in aqueous medium; therefore, sodium salt of ALA was used for the preparation of ALA aqueous solution, using the reported method [13].

**Table 1** Thermodynamic parameters.

Temperature $T$ (K)	Activation energy $E_a$ (kJ/mol)	Frequency factor $A$ (1/s) $\times 10^5$	Enthalpy $\Delta H^\circ$ (kJ/mol)	Entropy $\Delta S^\circ$ (kJ/mol)	Gibbs energy $\Delta G^\circ$ (kJ/mol)	Microstates $W$
<i>Thermodynamic parameters of ALA</i>						
302	36.7	1.28	34.82	−157.0	82.5	$6.5 \times 10^{-69}$
307				−157.5	83.2	
313				−157.8	84.2	
319				−157.8	85.2	
<i>Thermodynamic parameters of ALA with <math>Fe^{2+}</math></i>						
302	48	0.0191	47.82	−119.1	83.0	$2.08 \times 10^{-52}$
307				−120.5	84.0	
313				−119.2	85.0	
<i>Thermodynamic parameters of ALA with <math>Mo^{6+}</math></i>						
291	18	560	16.84	−206.8	77.0	$3.43 \times 10^{-90}$
297				−206.7	78.2	
302				−206.6	79.2	
308				−206.8	80.5	
<i>Thermodynamic parameters of ALA with synergistic effects</i>						
285	36.5	0.4	22.51	−188.7	76.2	$2.2 \times 10^{-82}$
292				−189.0	77.7	
302				−188.7	79.5	

### 2.3.1. Kinetic run

Experiments were performed at pH range from 4–10. A concentration of ALA solution in a mixture was  $4.89 \times 10^{-3}$  M and  $\text{H}_2\text{O}_2$  concentration  $9.325 \times 10^{-3}$  M. A required volume of solutions was mixed in a fixed proportion and the temperature was adjusted at  $29^\circ\text{C}$ . kinetic run was pursued by measuring absorbance of a mixture of thermo stated solute ions as a function of time at regular 180 s intervals up to 30–45 min. Absorbance readings were collected till the initial absorbance becomes half of its value in a quartz cell against a water blank. All experiments were performed at  $\lambda_{\text{max}}$  333 nm. For the catalyzed and other experiments similar runs were performed in the presence of particular metals keeping the other conditions constant.

## 3. Result and discussion

### 3.1. Effects of operating parameters

#### 3.1.1. Kinetic modeling

At specified experimental conditions different kinetic runs were performed and kinetic model was proposed accordingly.

#### 3.1.2. Effects of ALA concentration

Under pseudo first order conditions  $[\text{H}_2\text{O}_2] \gg [\text{ALA}]$  at a constant temperature  $29^\circ\text{C}$  and pH 7, plot of  $\ln$  Absorbance vs. time was linear ( $R^2 = 0.9992$ ), indicating a first order dependence on  $[\text{ALA}]$ . The plot of  $k'$  vs.  $[\text{ALA}]$  (ALA concentration varied from 2 to 9 mmol/L) indicates its degradation rate dependence on  $[\text{ALA}]$  (Fig. 1).

#### 3.1.3. Effects of $\text{H}_2\text{O}_2$ concentration

Under pseudo first order conditions  $[\text{H}_2\text{O}_2] \ll [\text{ALA}]$  at a constant temperature  $29^\circ\text{C}$  and pH 7, plot of  $\ln$  Absorbance vs. time was linear ( $R^2 = 0.9999$ ), indicating the first order dependence on  $[\text{H}_2\text{O}_2]$ . The plot of  $k'$  vs.  $[\text{H}_2\text{O}_2]$  ( $\text{H}_2\text{O}_2$  concentration varied from 9 to 74 mmol/L) indicates its degradation rate dependence on  $[\text{H}_2\text{O}_2]$ . Hence, the rate of degradation of ALA depends on a variation of both  $[\text{H}_2\text{O}_2]$  and  $[\text{ALA}]$  thus over all order of reaction is a second order (Fig. 2).

#### 3.1.4. Effects of pH

The degradation was also monitored over a pH range of 4–10 and the result is manifested in Fig. 3. The observed degradation rate of ALA indicates that the degradation is promising at neutral pH. The pH slightly changes the rate of reaction, but still order is independent of pH. To investigate its further effect, a series of experiments were performed at varying pH. It was found that the rate of a reaction is minimum at pH 6, maximum at 9 and at other pH ranges a reaction rate has shown a slight change.

### 3.2. Effect of metals

A number of metals were tried with a title reaction, to monitor the effect on the degradation of ALA. A wide range of mono, di, tri cations of Se, Co, Cr, Fe, Zn were investigated at two different pH. Out of them few were essential while others were non-essentials. Mo and Cd as a non-essential metal were tested in in vitro conditions. Among them,  $\text{Fe}^{2+}$  and  $\text{Mo}^{6+}$  were

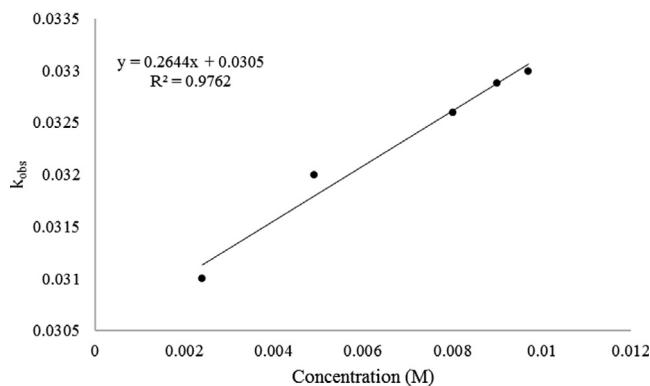


**Figure 1** Plot of varying concentrations of ALA against  $k_{\text{obs}}$  under pseudo-first order condition, at pH 7 keeping the temperature and other conditions constant, at all concentrations.

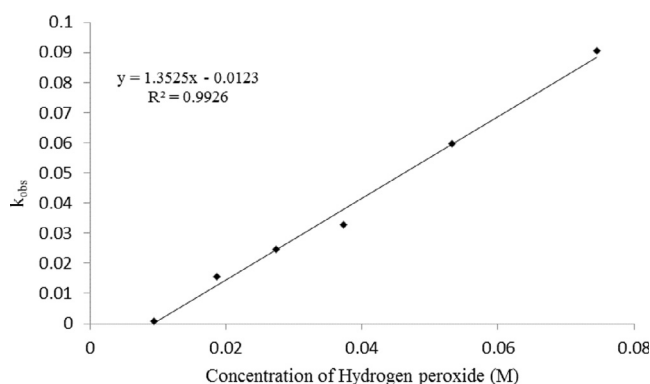


**Figure 2** Plot of hydrogen peroxide concentration against  $k_{\text{obs}}$  under pseudo first order condition, at pH 7 keeping the temperature and other conditions constant, at all concentrations.

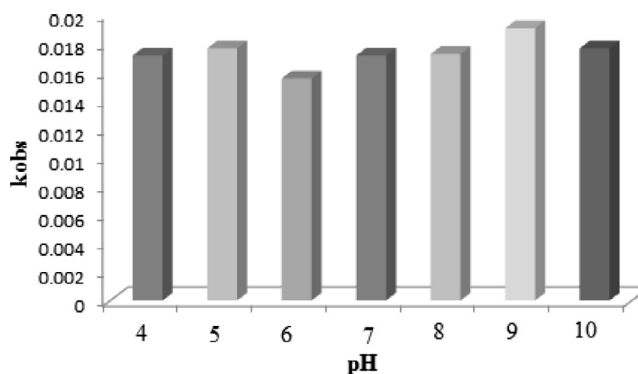


**Figure 3** Plot of  $k_{\text{obs}}$  vs. pH, there is a change in  $k_{\text{obs}}$  with the change in pH.

selected for further studies. The very reason for their selection is that Fe is abundantly available in the body and very important for the body functions and its interactions with  $\text{H}_2\text{O}_2$  [14]. The final selection of  $\text{Mo}^{6+}$  was based upon the prominent drastic change in reaction kinetics in comparison with the other metals used.

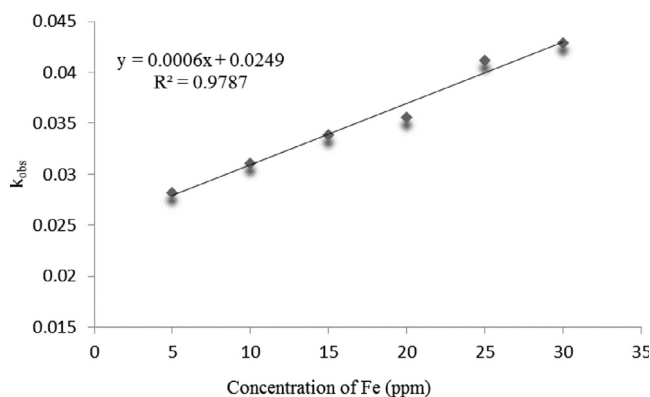


**Figure 4** Plot of  $[\text{Fe}^{2+}]$  vs.  $k_{\text{obs}}$  of the reaction at pH 6, temperature and other conditions were kept constant.

In the presence of  $\text{Fe}^{2+}$  the reaction mechanism of the degradation of ALA was changed. The rate was monitored at different  $\text{Fe}^{2+}$  concentrations and further its behavior at different temperatures was examined. ALA being a capping agent to Fe (II) [14] changes the degradation pathway of ALA and makes it stable against oxidizing agents such as  $\text{H}_2\text{O}_2$ . This chelation prevents it against the oxidative stress. As evident from Fig. 4 complexation is favored at low  $\text{Fe}^{2+}$  concentration while at higher concentrations a sharp change in reaction rate was observed, which is evident that instead of complexation, oxidation path is now followed.

### 3.3. Thermodynamic parameters

The effect of temperature on ALA degradation was studied at pH 4 and 6 from 24 to 46 °C the result indicates a rapid increase in  $k_{\text{obs}}$  with an increase in temperature at constant pH (Fig 5) as expressed by the Arrhenius equation:

$$k_{\text{obs}} = 1.28e^{-5} \exp(4333.3/T) \quad \text{at pH 6}$$

$$k_{\text{obs}} = 8.78e^{-5} \exp(3550.2/T) \quad \text{at pH 4}$$

The apparent activation energy was calculated to be 36 and 29.5 kJ/mol at pH 6 and 4 respectively.

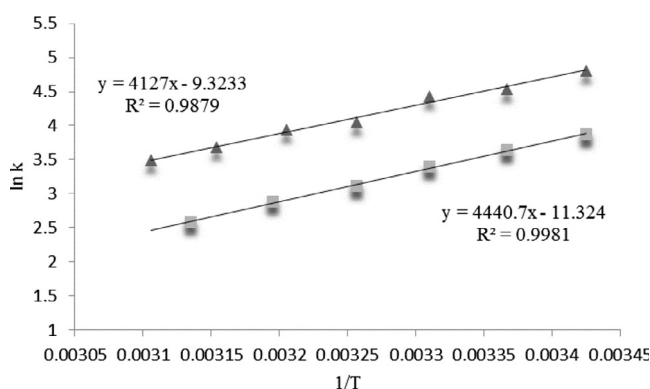


**Figure 5** Plot of reciprocal of temperature against  $\ln k$  produces activation energy plot, of ALA at  $\blacktriangle$  pH 4 and,  $\blacksquare$  pH6. The change in slope depicts the change in reaction path with the change of pH.

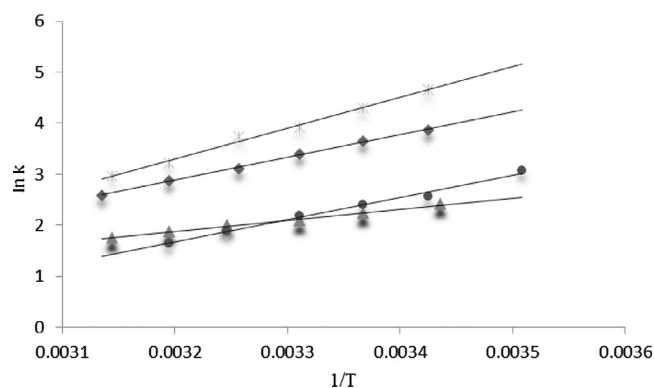


**Figure 6** Comparisons of activation energy plots of ALA with Fe, Mo and (Fe + Mo),  $\diamond Y = 4438.9x - 11.319$  ( $R^2 = 0.999$ ),  $*Y = 6038.2x - 16.027$  ( $R^2 = 0.9989$ ),  $\blacktriangle Y = 2181.1x - 5.0979$  ( $R^2 = 0.999$ ),  $\bullet Y = 4385.2x - 2.363$  ( $R^2 = 0.999$ ) respectively.

In the presence of  $\text{Mo}^{6+}$  (Catalyzed reaction) the change in slope is very promising at varying temperatures (Fig 6).

$$k_{\text{obs}} = 560e^{-5} \exp(2207.8/T) \quad \text{at pH 6}$$

The drop in activation energy from 36 kJ/mol to 18.3 kJ/mol, shows a promising change in reaction pathway, taking almost half the reaction time in its degradation.

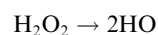
Whereas in the presence of an essential metal  $\text{Fe}^{2+}$  the effect of temperature on the reaction rate was studied by conducting kinetic runs at different temperatures (18–35 K) where other experimental conditions were kept similar. The Arrhenius plot of  $\ln k'$  vs.  $1/T$  was linear over a range ( $R^2 = 0.965$ ), (Fig. 6).

$$k_{\text{obs}} = 0.0191e^{-5} \exp(5861.8/T) \quad \text{at pH 6}$$

The activation energy of ALA changes from 36 to 48.7 kJ/mol which shows the relative stability of ALA against  $\text{H}_2\text{O}_2$  in the presence of  $\text{Fe}^{2+}$ . Different activation parameters ( $E_a$ ,  $\Delta H$ ,  $\Delta G$ ,  $\Delta S$ ,  $A$  and microstates) were calculated and mentioned in Table 1. These thermodynamic parameters were calculated by using following equation [15].

$$\frac{\Delta S}{R} = \ln \frac{k}{T} - \ln \left( \frac{\kappa k}{h} \right) + \frac{\Delta H}{RT}$$

The given values in Table 1 show that the said reaction is a non-spontaneous with respect to  $\Delta H$ ,  $\Delta S$ , and  $\Delta G$ . But, our observations show that it is a still perfectly favored reaction (i.e., spontaneous). As here  $\Delta G$  comes positive, which refers that the reaction is endergonic in nature. However, when we look closely into the initiation step of the reaction mechanism dissociation of the hydrogen peroxide takes place according to the following equation:



It is known that  $\text{H}_2\text{O}_2$  dissociates even at a very low temperature of 25 °C [16]. Thus, there is a strong possibility of coupling of this reaction with the primary reaction and in the result accumulating of free energy in highly active, short-lived intermediate  $\cdot\text{OH}$  during it attacks on ALA (second step of self-degradation Scheme (line 311)). This coupling of the reactions made these thermodynamically un-favored reactions into a favored one. Our reaction mechanism and that of calcu-

lated values are supporting the proposed justification about the reaction dynamics. In Table 1, the calculated microstates showed the possibility of molecular distribution. It increases as the entropy of the system increases or vice versa. The reported results supported the above argument.

### 3.3.1. Synergistic effect

As described earlier, the  $\text{Mo}^{6+}$  behaves as a catalyst and  $\text{Fe}^{2+}$  involves in the chelation, but when a mixture of these two was used in varying proportions, their reaction pathway gets changed. On analysis of the results by using combination software, the synergistic effect was found (Table 1, Fig. 7). Apparently it shows that they overcome the effect of each other. Whereas in case of synergistic working on a range of temperatures it gives the clear evidence of change in reaction pathway by the change of activation energy (Fig. 6).

$$k_{\text{obs}} = 0.4e^{-5} \exp(4400.3/T) \quad \text{at pH 6}$$

The plot of  $\ln k'$  vs.  $1/T$  ( $R^2 = 0.9959$ ) shows good agreement and this change in activation energy is quite promising. The obtained thermodynamic parameters for this reaction are also given in Table 2.

### 3.3.2. Salt effect

In order to propose the reaction mechanism, the salt effect was monitored by using potassium chloride (KCl) (0.01–0.35 M). The pseudo first order rate constant was calculated for different ionic strengths. Fig. 8 illustrates the varying trends in the slope due to the presence of salt effect. The positive slope for ALA was observed whereas the catalyzed and inhibited reactions indicate negative salt effect. The positive slope was observed in ALA degradation, (Fig. 8) whereas the opposite of this was observed in the presence of  $\text{Fe}^{2+}$  and  $\text{Mo}^{6+}$  which shows the change in reaction mechanism (Fig. 9).

### 3.3.3. Educated mechanism

Proposed mechanism of ALA degradation in the presence of  $\text{H}_2\text{O}_2$  may occur in the following manner.

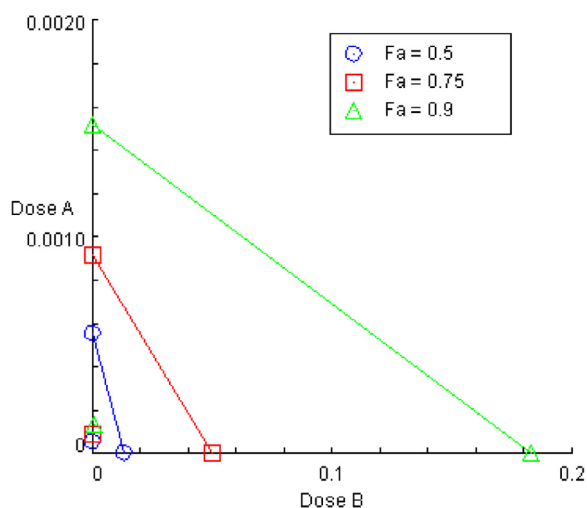
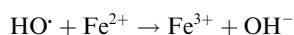
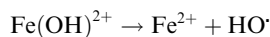
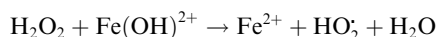
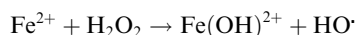


**Figure 7** Isobologram for combination of metals: Fe–Mo (Fe + Mo [1:5]). Fa represents the fraction affected.

**Table 2** Compusyn synergistic report results.

Total dose	Fa	CI value
<i>Iron 0.0000125 M the combination results are</i>		
3.75E–5	0.0035	1.96814
5.0E–5	0.0058	1.48896
6.25E–5	0.01	1.02294
7.5E–5	0.022	0.53249
<i>Iron 0.000025 the combination results are</i>		
3.75E–5	0.0024	2.74171
5.0E–5	0.0011	8.76667
6.25E–5	0.0071	1.4284
7.5E–5	0.0095	1.2716
8.75E–5	0.025	0.62075
<i>Iron 0.0000375 the combination results are</i>		
5.05E–5	7.0E–4	13.1621
6.25E–5	0.0055	1.78229
7.5E–5	0.0052	2.26291
8.75E–5	0.0134	1.06394
1.0E–4	0.0276	0.6508
<i>Iron 0.00005 the combination results are</i>		
6.25E–5	0.0025	3.78205
7.5E–5	0.0012	9.91225
8.75E–5	0.0047	2.80143
1.0E–4	0.0126	1.2895
1.13E–4	0.0248	0.83496
<i>Iron 0.0000625 the combination results are</i>		
7.5E–5	0.0058	1.85002
8.75E–5	0.0058	2.15836
1.0E–5	0.0025	5.39474
1.13E–4	5.0E–4	32.8947

It is reported that in the presence of  $\text{Fe}^{2+}$   $\text{H}_2\text{O}_2$  form  $\text{OH}^\cdot$  radical and hence speedup the degradation of ALA [14].



However, our results are contradicting the above scheme (Fig. 6 and Table 1).

Alternatively this is also reported that ALA chelates with  $\text{Fe}(\text{II})$  [7]. The increase in the value of activation energy of the oxidation reaction of  $\text{Fe}^{2+}$  confirmed the chelation of ALA with  $\text{Fe}(\text{II})$  as compared to oxidation of ALA via  $\text{OH}^\cdot$  free radical mechanism. In the chelated product, Fe is surrounded by three nine membered rings. The complex formed between Fe and ALA is in the ratio of 1:3 [7]. As a result  $\text{Fe}^{2+}$  becomes unavailable to react with  $\text{H}_2\text{O}_2$ , and due to high resonating structures, it becomes difficult for  $\text{H}_2\text{O}_2$  to degrade ALA because of strong stable chelation (Fig. 9).

ALA degradation in the presence of  $\text{Mo}^{6+}$  showed an opposite trend to that of  $\text{Fe}^{2+}$ . ALA oxidation reaction was performed in the presence of  $\text{Mo}^{6+}$  the other stable oxidation state of Mo is 4+. First ALA gets oxidized by  $\text{Mo}^{6+}$  and then  $\text{H}_2\text{O}_2$  oxidized it further, thus its degradation gets speed up as clearly evident from  $E_a$  value.



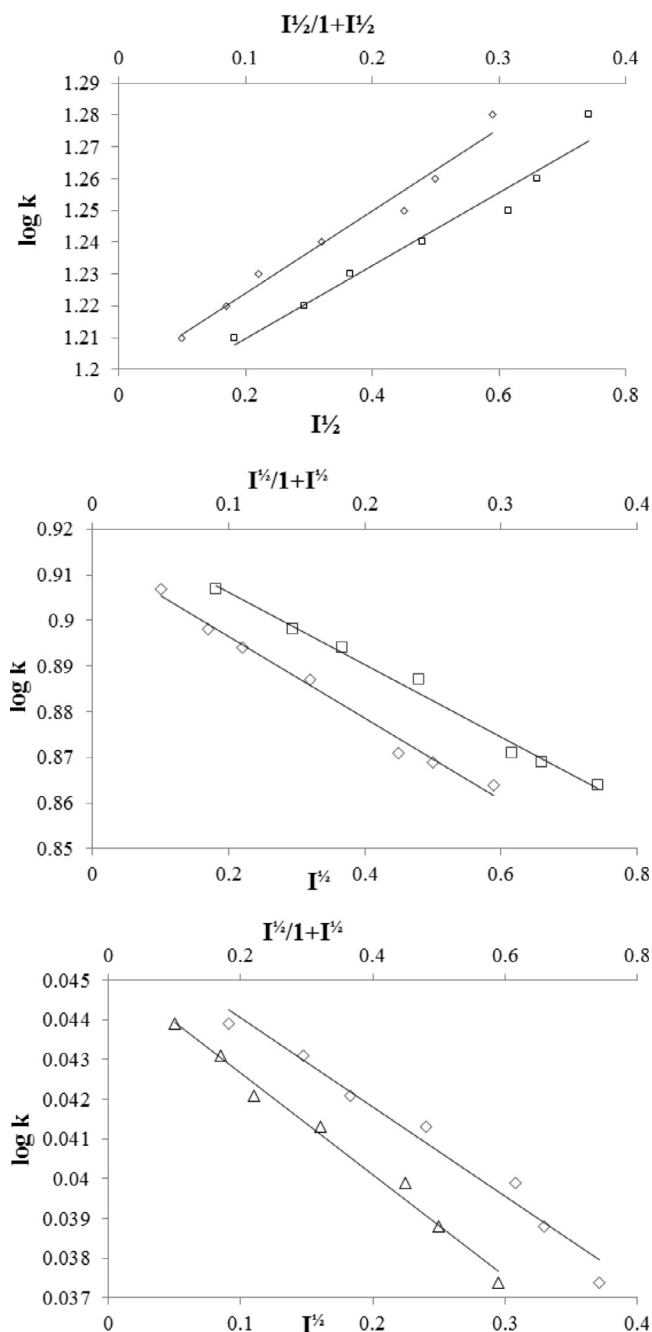
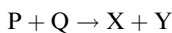


**Figure 8** KCl addition effect on the degradation rate of test reaction of ALA, the reaction as studied at pH 6 at room temperature. The effect was also monitored on catalyzed and inhibited reactions under the same conditions. Salt effect results of 1. ALA, 2. Mo, 3. Fe.



where P and Q are reacting species (P = ALA which is a monitoring specie, Q =  $\text{Mo}^{6+}$ ) X and Y are the products being formed as a result of degradation. On the basis of experimental observations following kinetic expression is suggested.

$$-\frac{d[P]}{dt} = k_u[P] + k_c[P][c] \quad (1)$$

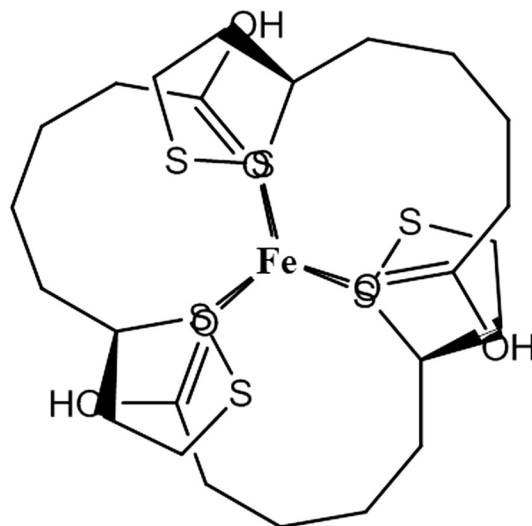


**Figure 9** Structural representation of Fe chelation with ALA.

$$-\frac{d[P]}{dt} = [P] + (k_u + k_c[c]_o) \quad (2)$$

In this  $k_u$  is the uncatalyzed rate coefficient whereas the  $k_c$  is the rate coefficient of catalyzed reaction, whereas  $[c]$  is the concentration of the catalyst which is  $\text{Mo}^{6+}$  in this case.

In order to dissect out the effects of all monitoring species, the concentrations of the reacting species were kept constant to make their effect on the rate, while the species being monitored is adjusted to first order dependence.



In all such reactions two major conditions were involved.

**Pre-equilibrium condition**

If  $k_1 \ll k_{-1}$  and  $k_2 \ll k_1$  the reaction represented in Eq. (4) is a rate determining step and Eq. (3) gives pre-equilibrium conditions:

$$[Pc] = k \frac{[c][p]}{[y]}$$

where  $k = \frac{k_{-1}}{k_1}$  is the equilibrium concentration and  $[P]_o$  and  $[c]_o$  are equilibrium concentrations at time  $t$ :

$$[P] = [P]_o - [(Pc)]$$

$$[c] = [c]_o - [(Pc)]$$

As  $c$  is a catalyst whose concentration is much lesser than that of  $P$  thus  $[P] \approx [P]_o$ .

$$[(Pc)] = \frac{k([c]_o - [(Pc)])[p]}{[y]}$$

$$[(Pc)] = \frac{k[c]_o[P_o - k][(Pc)][P]_o}{[y]}$$

$$[(Pc)][Y] = k[c]_o[P]_o - k[P]_o[(Pc)]$$

$$[(Pc)][Y] + k[(Pc)][P]_o = k[P]_o[c]_o$$

$$[(Pc)]([Y] + k[P]_o) = k[P]_o[c]_o$$

$$[(Pc)] = \frac{\kappa[c]_o[p]_o}{[y] + \kappa[p]_o}$$

Eq. (4) is a rate determining step in pre-equilibrium case

$$\text{Rate} = k_2[Pc][Q]$$

$$\text{Rate} = k_2[Q] \frac{\kappa[c]_o[p]_o}{[y] + \kappa[p]_o}$$

As the concentration of catalyst is very low in comparison with the reacting species, thus the concentration of  $Y$  formed is nearly negligible and concentration of the  $Q$  is constant,

$$\text{Rate} = \frac{d[p]}{dt} = \text{constant} \times [c]_o$$

OR

$$\text{Rate} = \frac{d[p]}{dt} = k'_2[c]_o \quad (k'_2 = k_2 \times \text{constant})$$

OR

$$\text{Rate} = \frac{d[p]}{dt} \propto [c]_o$$

$$\text{where } k'_2 = \frac{\kappa k_2[Q][p]_o}{k[p]_o}$$

The relationship between the catalyst concentrations to the proposed rate of reaction is clear from the above equation

Steady-state condition

If  $k_2 > k_1 > k_{-1}$  then reaction 3 becomes a rate determining step and  $[(Pc)]$  become small.

$$\frac{d[(Pc)]}{dt} = 0$$

Rate expression will be

$$\text{Rate} = k_1[P][c] - k_{-1}[(Pc)][Y]$$

As the concentration of  $[(Pc)]$  cannot be determined thus,

$$\frac{d[(Pc)]}{dt} = 0 = k_1[P][c] - k_{-1}[(Pc)][Y] - k_2[(Pc)][Q]^\circ$$

$$\frac{d[(Pc)]}{dt} = 0 = k_1[P][c] - k_{-1}[(Pc)][Y] - k_2[(Pc)]$$

Substituting the value of  $[P]$  as  $[P]_o$  and  $[c]$  as  $[c]_o - [(Pc)]$  (as  $P = [P]_o - [Pc] \approx [P]_o$ )  $[Pc]$  concentration is much larger than  $[P]_o$ .

$$0 = k_1[P]_o([c]_o - [(Pc)]) - k_{-1}[(Pc)][Y] - k_2[(Pc)]k_1[P]_o[c]_o$$

$$= [(Pc)](k_1[R]_o + k_{-1}[Y] + k_2)$$

$$[(Pc)] = \frac{\kappa_1[c]_o[P]_o}{k_1[P]_o + k_{-1}[Y] + k_2}$$

By putting the  $[(Pc)]$  value in this equation  $\text{Rate} = k_1[P][c] - k_{-1}[(Pc)][Y]$  we get

$$\text{Rate} = k_1[P][c] - k_{-1}[Y] \frac{k_1[c]_o[p]_o}{k_1[p]_o + k_{-1}[Y] + k_2}$$

As already mentioned  $[P] = [P]_o$  and  $[c] = [c]_o$ .

$$\text{Rate} = k_1[P]_o([c]_o - [Pc]) - k_{-1}[Y] \frac{k_1[c]_o[p]_o}{k_1[p]_o + k_{-1}[Y] + k_2}$$

$$\text{Rate} = k_1[P]_o[c]_o - k_1[P]_o \frac{k_1[c]_o[p]_o}{k_1[p]_o + k_{-1}[Y] + k_2}$$

$$- \frac{k_{-1}[Y]k_1[c]_o[p]_o}{k_1[p]_o + k_{-1}[Y] + k_2}$$

Rate

$$= \frac{k_1[c]_o[p]_o(k_1[p]_o + k_{-1}[Y] + k_2) - k_1^2[p]_o^2[c]_o - k_1k_{-1}[p]_o^2[c]_o[Y]}{k_1[p]_o + k_{-1}[Y] + k_2}$$

$$\text{Rate} = \frac{k_1k_2[c]_o[p]_o}{k_1[p]_o + k_{-1}[Y] + k_2}$$

As  $k_{-1}[Y] < k_1[P]$  thus

$$\text{Rate} = \frac{k_1k_2[c]_o[p]_o}{k_1[p]_o + k_2}$$

$$\text{Rate} = k'_2[c]_o$$

$$\text{Although } k't_2 = \frac{k_1k_2[p]_o}{k_1[p]_o + k_2}$$

$$\text{Rate} = \Delta[c]_o$$

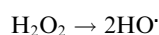
Equilibrium and a steady state gave a similar relationship and experimental proofs and further verify these relations.

But when both  $\text{Mo}^{6+}$  and  $\text{Fe}^{2+}$  added in combination, synergism was observed by using *Compusyn* software. This software is used to find the maximum dose effect in biomedical research studies but here it is used to find the combination effect of two metals. Changed behavior may be observed due to the fact that in the presence of  $\text{Fe}^{2+}$  degradation reaction follows some path having high resistance to completion of degradation and the reason is already discussed above. When degradation is observed in the presence of  $\text{Mo}^{6+}$ ; this leads the reaction path having a low barrier to cross for product formation so it is quite obvious that when they both are added in different combinations then as a result the activation energy is found to be the combination of the two reactions.

#### 4. Conclusions

ALA degradation was observed in the presence of the strong oxidizing agent, and this degradation increases many folds when  $\text{Mo}^{6+}$  is present, but degradation decreases many folds when with  $\text{Fe}^{2+}$ . The  $\text{UV}/\text{H}_2\text{O}_2$  treatment is the major degradation pathway. The synergistic effect was observed when both  $\text{Fe}^{2+}$  and  $\text{Mo}^{6+}$  are present in combination. The educated mechanism was proposed with the help of above results.

Self-degradation Scheme







- its initiation of stress signaling pathways that promote endogenous antioxidant capacity, *IUBMB Life* 60 (2008) 362–367.
- [8] A.J. Bush, Metal complexing agents as therapies for Alzheimer's disease, *Neurobiol. Aging* 23 (2002) 1031–1038.
- [9] N.M. Mahmoodi, M. Arami, N.Y. Limaee, N.S. Tabrizi, Decolorization and aromatic ring degradation kinetic of Direct Red 80 by UV oxidation in the presence of hydrogen peroxide utilizing  $\text{TiO}_2$  as a photocatalyst, *Chem. Eng. J.* 112 (2005) 191–196.
- [10] I. Mori, K. Takasaki, Y. Fujita, T. Matsuo, Selective and sensitive fluorometric determinations of cobalt (II) and hydrogen peroxide with fluorescein-hydrazide, *Talanta* 47 (1998) 631–637.
- [11] Y. Lee, M. Cho, J.Y. Kim, J. Yoon, Chemistry of ferrate (Fe(VI)) in aqueous solution and its applications as a green chemical, *J. Ind. Eng. Chem.* 10 (2004) 161–171.
- [12] A.A. Fatokun, T.W. Stone, R.A. Smith, Hydrogen peroxide-induced oxidative stress in MC3T3-E1 cells. The effects of glutamate and protection by purines, *Bone* 39 (2006) 542–551.
- [13] N. Perricone, K. Nagy, F. Horváth, G. Dajkó, I. Uray, I. Zs-Nagy, Alpha lipoic acid (ALA) protects proteins against the hydroxyl free radical-induced alterations: rationale for its geriatric topical application, *Arch. Gerontol. Geriatr.* (1999).
- [14] Y.F. Sun, J.J. Pignatello, Photochemical reactions involved in the total mineralization Of 2, 4-D by  $\text{Fe}^{3+}/\text{H}_2\text{O}_2/\text{UV}$ , *Environ. Sci. Technol.* 27 (1993) 304–310.
- [15] R.W. Margaret, *An Introduction to Chemical Kinetics*, first ed., John Wiley and Sons, England, 2004.
- [16] M.N. Tofik, *Coherent Synchronized Oxidation Reactions by Hydrogen Peroxide*, first ed., Elsevier, Netherlands, 2007.